

# Research

## 3D Printing—Article

# Bioprinting-Based High-Throughput Fabrication of Three-Dimensional MCF-7 Human Breast Cancer Cellular Spheroids

Kai Ling<sup>1,2</sup>, Guoyou Huang<sup>2,3</sup>, Juncong Liu<sup>2</sup>, Xiaohui Zhang<sup>2,3</sup>, Yufei Ma<sup>2,3</sup>, Tianjian Lu<sup>2\*</sup>, Feng Xu<sup>2,3\*</sup>

**ABSTRACT** Cellular spheroids serving as three-dimensional (3D) *in vitro* tissue models have attracted increasing interest for pathological study and drug-screening applications. Various methods, including microwells in particular, have been developed for engineering cellular spheroids. However, these methods usually suffer from either destructive molding operations or cell loss and non-uniform cell distribution among the wells due to two-step molding and cell seeding. We have developed a facile method that utilizes cell-embedded hydrogel arrays as templates for concave well fabrication and *in situ* MCF-7 cellular spheroid formation on a chip. A custom-built bioprinting system was applied for the fabrication of sacrificial gelatin arrays and sequentially concave wells in a high-throughput, flexible, and controlled manner. The ability to achieve *in situ* cell seeding for cellular spheroid construction was demonstrated with the advantage of uniform cell seeding and the potential for programmed fabrication of tissue models on chips. The developed method holds great potential for applications in tissue engineering, regenerative medicine, and drug screening.

**KEYWORDS** MCF-7 cellular spheroids, bioprinting, hydrogels, concave wells, tissue on a chip

## 1 Introduction

*In vitro* tissue models such as those based on cellular spheroids have attracted increasing interest in cellular biology, tissue engineering, regenerative medicine, and drug-screening applications [1–4]. Cellular spheroids are three-dimensional (3D) aggregates of multi-cells, which usually scale from tens to hundreds of micrometers. It is widely accepted that cells in cellular spheroids behave and respond to changes in mi-

croenvironment cues in a much more natural manner than those on traditional two-dimensional (2D) culture plates [5, 6]. In addition, cellular spheroids are inherently scaffold free as compared to scaffold-based 3D models; this property may help cellular spheroids to avoid biocompatibility issues [7]. Different types of cells have been engineered into cellular spheroids, including normal [8, 9], cancerous [10, 11], and stem cells [12, 13], as well as a mixture of cell types [14, 15]. In particular, the introduction of chip technologies has recently inspired the emergence and prominent development of tissue/organ-on-a-chip technology, which is believed to hold great promise in biomedical fields [16–18].

Various methods have been developed for generating cellular spheroids by exploring the fluidic and self-assembly abilities of cells [19]. A facile method is to culture cells on non-adherent substrates [20], where the cell-cell interaction is stronger than that of cell-substrate, resulting in the aggregation of cells. To promote the assembly of cells, gravitational and magnetic forces have been explored, leading to the development of the hanging-drop [21] and magnetic-levitation methods [22], respectively. Microwells have also been widely used to confine the growth space of cells with the benefit of forming cellular spheroids with controlled and uniform size [11]. Among these methods, microwells have attracted increasing attention; especially those with concave structures, due to advantages such as easy operation, good controllability, and high-throughput capacity [23, 24]. However, almost all of the current microwell methods require the manual seeding of cells after the preparation of a microwell plate, which may be cumbersome and can cause cell loss and non-uniform cell seeding [25]. In addition, special templates and a careful molding process are required to obtain well-defined concave microwells, which limits their accessibility. Therefore, there

<sup>1</sup> State Key Laboratory for Strength and Vibration of Mechanical Structures, School of Aerospace, Xi'an Jiaotong University, Xi'an 710049, China; <sup>2</sup> Bioinspired Engineering and Biomechanics Center (BEBEC), Xi'an Jiaotong University, Xi'an 710049, China; <sup>3</sup> The Key Laboratory of Biomedical Information Engineering of the Ministry of Education, School of Life Science and Technology, Xi'an Jiaotong University, Xi'an 710049, China

\* Correspondence authors. E-mail: tjlu@mail.xjtu.edu.cn, fengxu@mail.xjtu.edu.cn

Received 9 February 2015; received in revised form 25 March 2015; accepted 30 March 2015

is still an urgent need for a flexible manufacturing method for fabricating cellular spheroids, particularly those with the potential for engineering tissues on chips.

In this study, we developed a bioprinting-based method for fabricating concave wells and generating cellular spheroids *in situ* on a chip. A custom-built bioprinting system was first constructed and applied in order to generate cell-laden sacrificial gelatin arrays. These cell-laden gelatin arrays were subsequently used as templates for fabricating concave wells and forming cellular spheroids on a non-adhesive hydrogel substrate. The method is facile and, to the best of our knowledge, represents the first use of biocompatible hydrogels as templates for fabricating concave wells with *in situ* cell-seeding ability for cellular spheroid formation.

## 2 Materials and methods

### 2.1 Set-up and improvement of the bioprinting system

To get high controllability for the droplet generation of gelatin sol, a pressure-assisted value-based bioprinting system was applied. This system was custom built, and is shown in Figure 1(a). The system was set up in a vertical laminar-flow clean workbench, with the main components being a three-axis motion stage (KDT180-100-LM (XY) and MT105-50-LM (Z), Feinmess Dresden GmbH, Dresden, Germany), a solenoid valve ejector (Model G100-150300, TechElan, Mountainside, NJ, USA), and a digital signal generator (Agilent 81101A, Test Equipment Connection, Lake Mary, FL, USA). All of these components were controlled using a computer.

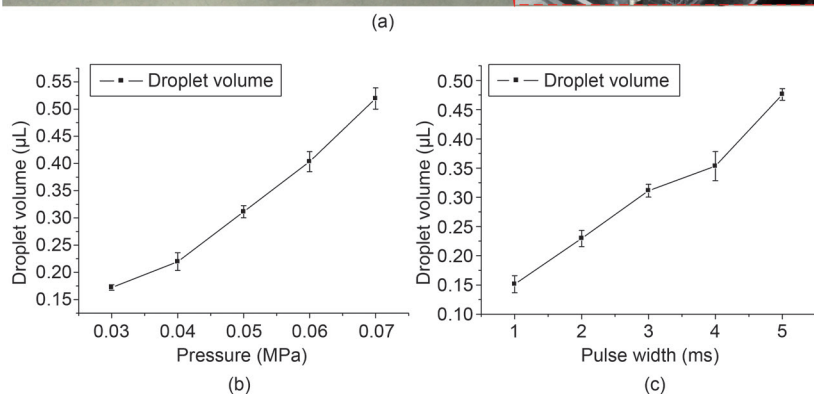
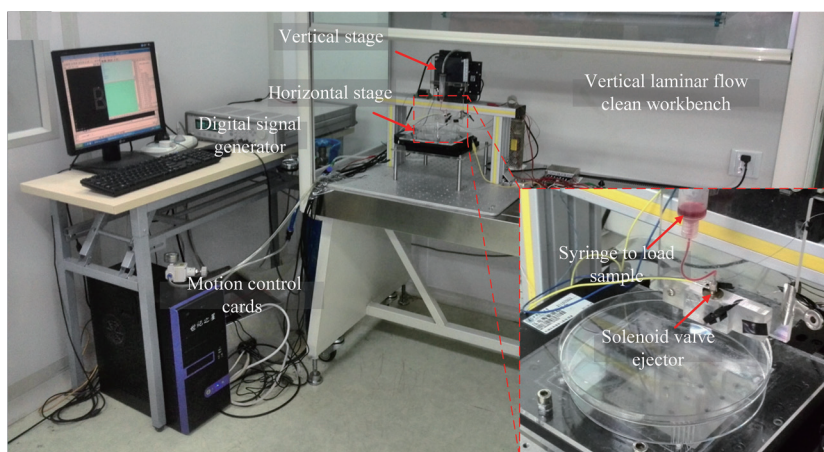


**Figure 1. Bioprinting platform.** (a) Image of the bioprinting platform; (b) mean droplet volume as a function of pneumatic pressure, and the valve-opening duration is 5 ms; (c) mean droplet volume as a function of valve-opening duration, and the pneumatic pressure is 0.05 MPa. Error bars represent standard error ( $n = 5$ ).

### 2.2 Bioprinting-based fabrication of sacrificial gelatin arrays

Gelatin was chosen for the sacrificial hydrogel arrays due to its biocompatibility and its injectable and reversible gelling abilities under mild temperature conditions. To fabricate the gelatin arrays, porcine-skin gelatin powder (gel strength 300, Type A, Sigma-Aldrich, St. Louis, MO, USA) was added to a phosphate-buffered sa-

line (PBS) solution at a concentration of 3% (w/v) and gently stirred at 50 °C until fully dissolved. The sol solution was then water-bathed to 37 °C, transferred to the sample-holding syringe, and printed onto a culture petri dish coated with a polytetrafluoroethene (PTFE) membrane. The PTFE membrane was used because it is physically hydrophobic and chemically inert, as well as easy to use. The temperature of the gelatin solution in the syringe was kept at 37 °C during printing. The assisted printing pressure and pulse width of the signal were adjusted to control the printed volume of the gelatin droplet and thus the size and shape of the gelatin arrays. The petri dish with the printed gelatin arrays was immediately transferred to a refrigerator and cooled at 4 °C for 5 min in order to gel the gelatin precursor.

### 2.3 Gelatin-array templated fabrication of concave wells

Polyethylene glycol (PEG)-based hydrogels were used to mold concave wells from gelatin arrays due to their biocompatibility, photocrosslinkability, and cell-nonadhesive properties. These hydrogels have also been used by others to fabricate wells for the formation of cellular spheroids [26–28]. In our experiment, PEG-dimethacrylate (PEG-DMA, MW 1000, Polysciences, Inc., Warrington, PA, USA) was dissolved in a PBS solution at a concentration of 20% (w/v) and then cooled to 4 °C. After being poured onto the petri dish with the gelatin arrays, the PEG-DMA solution was exposed to 365 nm ultraviolet (UV) light with a power of 2.9 mW·cm<sup>-2</sup> (Model XLE-1000 A/F, Spectroline, Westbury, NY, USA) for 20 s for gelling. During the photocrosslinking, 2-hydroxy-2-methylpropiophenone (TCI Shanghai Development Co., Ltd., Shanghai, China) was used as the photoinitiator at a concentration of 0.1% (w/v). After incubation at 37 °C for 24 h, the gelatin arrays redissolved into a sol phase and concave wells formed on the PEG-DMA substrate.

### 2.4 Characterization of gelatin arrays and concave wells

The gelatin arrays were imaged with an inverted fluorescence microscope (Olympus IX 81, Olympus, Irvine, CA, USA) before molding with PEG-DMA.

To image the wells, the PEG-DMA substrate was gently detached from the PTFE-covered petri dish, and swelled to equilibrium in a PBS solution. After being taken out of the PBS solution, the excess PBS solution on the PEG-DMA substrate surface and in the wells was gently removed with blotting paper. To capture a cross-section of the wells, the PEG-DMA substrate was carefully cut through the wells with a razor blade and images were immediately taken with an IX 81 microscope. The images were analyzed with Image-Pro Plus (IPP, version 6.0, Media Cybernetics, Silver Spring, Rockville, MD, USA) to quantify the sizes of the gelatin arrays and wells on the PEG-DMA substrate.

### 2.5 *In situ* cell seeding and cellular spheroid formation

We used MCF-7 human breast cancer cells to verify the *in situ* cell-seeding ability of our method for the high-throughput fabrication of cellular spheroids on a chip. Cells were cultured in RPMI 1640 medium (HyClone, South Logan, UT, USA) and supplemented with 10% fetal bovine serum (Gibco Industries, Inc., Big Cabin, OK, USA) in a humidified 5% CO<sub>2</sub> incubator at 37 °C. Before the experiment, the cells were digested with trypsin (EDTA 1×, Mediatech, Inc., Manassas, VA, USA) and centrifuged, and the liquid supernatant was removed. The cells were then resuspended in the culture medium. The prepared cellular suspension was then gently mixed with a pre-filtered gelatin solution at a final cell density of  $5 \times 10^5$  cells·mL<sup>-1</sup> to  $1 \times 10^6$  cells·mL<sup>-1</sup> and a gelatin concentration of 3% (w/v) at 37 °C. The cell-gelatin mixture was then loaded into the syringe for the fabrication of the gelatin arrays and wells as described in Sections 2.2 and 2.3. The petri dish cover was removed after incubation for 1 h and the cell culture medium was changed daily. Phase-contrast images of the cellular spheroids were observed with an Olympus IX 81. Confocal fluorescence images (LSM700, ZEISS, New York, NY, USA) were observed after the spheroids or aggregates were stained using a live/dead viability/cytotoxicity kit (Invitrogen, Washington, DC, USA). The kit stained live cells green with calcein AM and dead cells red with ethidium homodimer-1. Cell viability was quantified from confocal slices using IPP.

## 3 Results and discussion

The bioprinting system we constructed is shown in Figure 1(a). High controllability of the bioprinting system for producing droplets of nL volume was demonstrated; this controllability can be achieved by changing the pneumatic pressure or the valve-opening duration, as shown in Figure 1(b) and Figure 1(c), respectively. The optimized concentration of the gelatin sol solution was found to be ~3% (w/v), below which the gelatin arrays were too soft to be used as templates and above which valve blocking and solution ponding occurred.

The bioprinting system was then applied to produce controlled gelatin arrays for fabricating concave wells and *in situ* cellular spheroid formation, as illustrated in Figure 2. First, gelatin arrays of different sizes were created on a hydrophobic PTFE-covered petri dish, as shown in Figure 3(a–c). After molding, concave wells were formed on the PEG-

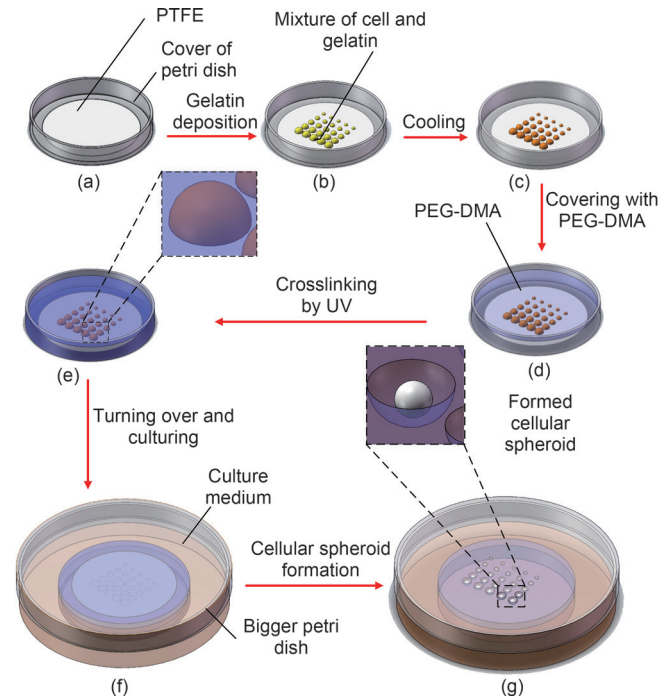


**Figure 2. Schematics of concave-well fabrication and *in situ* cell seeding for cellular spheroid formation.** (a) Cover the petri dish with a film layer of hydrophobic PTFE; (b) print gelatin and cell solution onto PTFE-covered petri dish; (c) cell-encapsulated hydrogel array forms when cooled at 4 °C; (d) pour the cold PEG-DMA solution onto the cell-encapsulated gelatin array and (e) expose it to UV light for crosslinking; (f) turn it over and incubate at 37 °C to liquefy the gelatin and release cells onto the well bottom; (g) cellular spheroids form during further culture.

DMA substrate with almost the same size as the gelatin-array templates, as shown in Figure 3(d–f), demonstrating the high molding fidelity and thus the feasibility of using gelatin arrays as templates. By tuning the volume of the printed gelatin droplets from 0.1  $\mu$ L to 0.48  $\mu$ L, gelatin arrays with a radius ranging from 420  $\mu$ m to 530  $\mu$ m and a depth ranging from 230  $\mu$ m to 550  $\mu$ m can be easily obtained, as shown in Figure 3(g). This method led to the formation of concave wells with a radius ranging from 480  $\mu$ m to 530  $\mu$ m and a depth ranging from 250  $\mu$ m to 550  $\mu$ m, as shown in Figure 3(h). The droplet volume can be easily tuned by adjusting either the printing pressure or the pulse width of the digital signal. Since high pressure may lead to cell damage and an unwantedly forceful impact between the gelatin droplet and the substrate, we only tuned the pulse signal width to control the gelatin droplet volume. Wells with a high depth may have the advantage of avoiding cell loss during the medium exchange. We expect that wells with a much more controlled size and a higher molding fidelity could be fabricated by optimizing the production of the gelatin arrays, which may be achieved by improving the gelatin droplet hydrophobic angle by use of more hydrophobic substrates.

To prove the *in situ* cell-seeding ability of our method for cellular spheroid formation on a chip, we first mixed MCF-7 cells with a gelatin precursor at a density of  $1 \times 10^6$  cells·mL<sup>-1</sup> and printed the mixture at a volume of 0.48  $\mu$ L per droplet. After molding and incubation at 37 °C for 1 h, the gelatin arrays reversed to the sol phase and the cells, encapsulated in gelatin, were released and deposited onto the bottom of

wells formed on the PEG-DMA substrate. During the subsequent culture, the cells proliferated, huddled together, and finally self-assembled into compacted cellular

spheroids on the 7th day, as shown in Figure 4(a). We observed very few dead cells throughout the process, as shown in Figure 4(b). Cellular spheroid formation with a printed volume of 0.23  $\mu\text{L}$  and the same cell-seeding density (i.e.,  $1 \times 10^6$  cells·mL<sup>-1</sup>) was also studied. Although cellular aggregates were observed after 7 days of culture, these were not as compacted as those in the 0.48  $\mu\text{L}$  group, as shown in Figure 4(c). The observed cellular aggregates did not change notably even after 14 days of culture (results not shown here). The horizontal cross-sectional confocal fluorescence image in Figure 4(b) shows that there is a black central domain without stained cells, which may be induced by diffusion limitation of the live/dead solution in compacted cellular spheroids. This central domain is not observed in Figure 4(d), indicating that the formed cellular aggregates with a printed gelatin volume of 0.23  $\mu\text{L}$  may be in a disk shape. From Figure 3(f) and Figure 3(h), we know that the fabricated wells with printed gelatin volumes of 0.23  $\mu\text{L}$  and 0.48  $\mu\text{L}$  per droplet have radiuses of 480  $\mu\text{m}$  and 530  $\mu\text{m}$ , and depths of 390  $\mu\text{m}$  and 550  $\mu\text{m}$ , respectively. Thus, it seems to us that well depth may play an important role in the formation of compacted cellular spheroids.

We further investigated the influence of initial *in situ* cell-seeding density

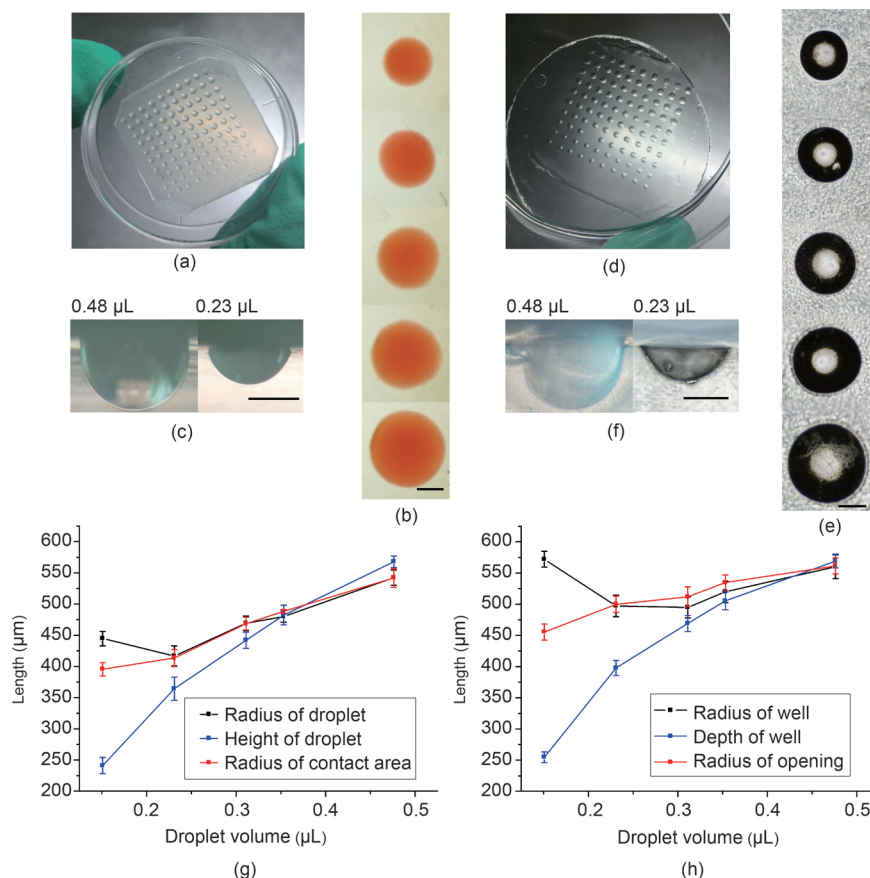


**Figure 3. Controlled fabrication of hydrogel concave wells.** (a) Overall view of printed gelatin arrays of different sizes on a PTFE-covered petri dish; (b) top-view microscope image of the gelatin arrays; (c) side view of two typical gelled gelatin droplets; (d) overall view of concave wells formed on PEG-DMA; (e) top-view microscope image of PEG-DMA wells; (f) side view of the cross-section of the concave wells; (g) controllability of the sizes of gelatin arrays; (h) controllability of the sizes of concave wells. Scale bars in (b), (c), (e), and (f) are 0.5 mm. Error bars in (g) and (h) represent standard deviation ( $n = 5$ ).

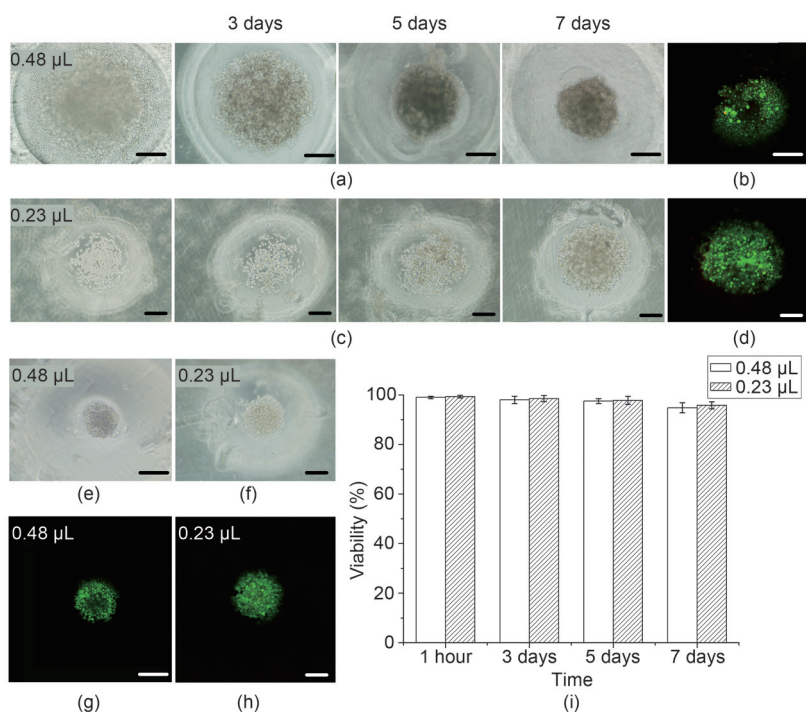


**Figure 4. Cellular spheroid formation in hydrogel concave wells.** (a) Phase-contrast images of cellular spheroid development and (b) calcein and ethidium bromide staining of cells after 7 days of culture in wells made of 0.48  $\mu\text{L}$  gelatin droplets and with a cell-seeding density of  $1 \times 10^6$  cells·mL<sup>-1</sup>; (c) phase-contrast images of cellular spheroid development and (d) calcein and ethidium bromide staining of cells after 7 days of culture in wells made of 0.23  $\mu\text{L}$  gelatin droplets and with a cell-seeding density of  $1 \times 10^6$  cells·mL<sup>-1</sup>; (e, f) phase-contrast images of cellular spheroid formation after 7 days of culture in wells made of (e) 0.48  $\mu\text{L}$  and (f) 0.23  $\mu\text{L}$  gelatin droplets, with a cell-seeding density of  $5 \times 10^5$  cells·mL<sup>-1</sup>; (g, h) live/dead fluorescence images corresponding to (e) and (f), respectively; (i) cell viability during cellular spheroid formation. Scale bars in (a)–(h) are 200  $\mu\text{m}$ .

on the formation of cellular spheroids. The results clearly showed that much smaller cellular spheroids were formed at a cell-seeding density of  $5 \times 10^5$  cells·mL<sup>-1</sup>, as shown in Figure 4(e)–(h), compared to a density of  $1 \times 10^6$  cells·mL<sup>-1</sup>, as shown in Figure 4(a)–(d). Therefore, it is possible to control the size of cellular spheroids by adjusting the *in situ* cell-seeding density. Figure 4(i) shows that high cell viability was maintained during cellular spheroid formation. In addition, cell loss was effectively avoided with the *in situ* cell-seeding ability. Moreover, uniform distribution of seeded cells between wells was achieved due to the controllability of the bioprinting system. Morphologically speaking, cellular spheroids can better mimic the structure of organoids and thus the microenvironment of cancer cells *in vivo* than can traditional 2D culture plates. It is therefore expected that MCF-7 may behave similarly in cellular spheroids and *in vivo*. To demonstrate this, further studies including a drug test are needed; these will be our next work. Although we only tested MCF-7 cells here, we believe that other cell types can be used, since gelatin has been widely applied for cell encapsulation and since a polyethylene glycol (PEG) hydrogel-based well plate has been successfully used for producing cellular spheroids of various cell types, including embryonic stem cells [29, 30].

Several researchers have demonstrated the use of molded or printed gelatin sacrificial elements for fabricating microfluidic hydrogels. In this work, we employed gelatin arrays as templates for the first time to generate concave wells for cellular spheroid formation. Although other templates, including solid resin mold, SU-8, polydimethylsiloxane (PDMS), and ice array, have been developed for fabricating concave wells, these methods suffer from either cumbersome mold preparation or destructive demolding operations [23, 31–33]. In addition, the post manual cell-seeding step may cause cell loss and non-uniform cell distribution. Here, by using a biocompatible and temperature-reversible cell-laden gelatin-array template, we provide a possible solution to overcome the above limitations. Moreover, the use of a custom-built bioprinting system may enable us to fabricate cellular spheroids *in situ* on a chip in a controlled and high-throughput manner, which will be of great help in engineering tissues on chips.

## 4 Conclusions

This work demonstrated the fabrication of concave wells molded from a hydrogel array with *in situ* seeding of cells for cellular spheroid formation on a chip. The use of a custom-built bioprinting approach endows the method with high controllability and a high-throughput capacity. The integration of bioprinting and *in situ* cell seeding with gelatin may enable highly programmed fabrication of cells/tissues on chips, and thus holds great promise for tissue engineering, regenerative medicine, and drug-screening applications.

## Acknowledgements

This work was financially supported by the National Natural Science Foundation of China (11372243, 11532009,

and 11522219), the China Postdoctoral Science Foundation (2013M540742), the Doctoral Program of Higher Education of China (201302011120071), the Natural Science Basic Research Plan in Shaanxi Province of China (2014Q1004), and the Fundamental Research Funds for the Central Universities.

## Compliance with ethics guidelines

Kai Ling, Guoyou Huang, Juncong Liu, Xiaohui Zhang, Yufei Ma, Tianjian Lu, and Feng Xu declare that they have no conflict of interest or financial conflicts to disclose.

## References

1. T. M. Achilli, J. Meyer, J. R. Morgan. Advances in the formation, use and understanding of multi-cellular spheroids. *Expert Opin. Biol. Ther.*, 2012, 12(10): 1347–1360
2. M. Rimann, U. Graf-Hausner. Synthetic 3D multicellular systems for drug development. *Curr. Opin. Biotechnol.*, 2012, 23(5): 803–809
3. L. Wang, et al. Engineering three-dimensional cardiac microtissues for potential drug screening applications. *Curr. Med. Chem.*, 2014, 21(22): 2497–2509
4. J. Rouwkema, J. de Boer, C. A. van Blitterswijk. Endothelial cells assemble into a 3-dimensional prevascular network in a bone tissue engineering construct. *Tissue Eng.*, 2006, 12(9): 2685–2693
5. E. Fennema, N. Rivron, J. Rouwkema, C. van Blitterswijk, J. de Boer. Spheroid culture as a tool for creating 3D complex tissues. *Trends Biotechnol.*, 2013, 31(2): 108–115
6. K. Takayama, et al. 3D spheroid culture of hESC/hiPSC-derived hepatocyte-like cells for drug toxicity testing. *Biomaterials*, 2013, 34(7): 1781–1789
7. P. R. Baraniak, T. C. McDevitt. Scaffold-free culture of mesenchymal stem cell spheroids in suspension preserves multilineage potential. *Cell Tissue Res.*, 2012, 347(3): 701–711
8. A. P. Napolitano, et al. Scaffold-free three-dimensional cell culture utilizing micromolded nonadhesive hydrogels. *Biotechniques*, 2007, 43(4): 494, 496–500
9. D. M. Dean, J. R. Morgan. Cytoskeletal-mediated tension modulates the directed self-assembly of microtissues. *Tissue Eng. Part A*, 2008, 14(12): 1989–1997
10. J. Liu, et al. Soft fibrin gels promote selection and growth of tumorigenic cells. *Nat. Mater.*, 2012, 11(8): 734–741
11. J. Friedrich, C. Seidel, R. Ebner, L. A. Kunz-Schughart. Spheroid-based drug screen: Considerations and practical approach. *Nat. Protoc.*, 2009, 4(3): 309–324
12. H. F. Chan, Y. Zhang, Y. P. Ho, Y. L. Chiu, Y. Jung, K. W. Leong. Rapid formation of multicellular spheroids in double-emulsion droplets with controllable microenvironment. *Sci. Rep.*, 2013, 3: 3462
13. F. Langenbach, et al. Generation and differentiation of microtissues from multipotent precursor cells for use in tissue engineering. *Nat. Protoc.*, 2011, 6(11): 1726–1735
14. M. Inamori, H. Mizumoto, T. Kajiwara. An approach for formation of vascularized liver tissue by endothelial cell-covered hepatocyte spheroid integration. *Tissue Eng. Part A*, 2009, 15(8): 2029–2037
15. S. F. Wong, D. Y. No, Y. Y. Choi, D. S. Kim, B. G. Chung, S. H. Lee. Concave microwell based size-controllable hepatosphere as a three-dimensional liver tissue model. *Biomaterials*, 2011, 32(32): 8087–8096
16. D. Huh, B. D. Matthews, A. Mammoto, M. Montoya-Zavala, H. Y. Hsin, D. E. Ingber. Reconstituting organ-level lung functions on a chip. *Science*, 2010,

- 328(5986): 1662–1668
17. D. Huh, Y. S. Torisawa, G. A. Hamilton, H. J. Kim, D. E. Ingber. Microengineered physiological biomimicry: Organs-on-chips. *Lab Chip*, 2012, 12(12): 2156–2164
  18. G. Wang, et al. Modeling the mitochondrial cardiomyopathy of Barth syndrome with induced pluripotent stem cell and heart-on-chip technologies. *Nat. Med.*, 2014, 20(6): 616–623
  19. R. A. Rezende, et al. Scalable biofabrication of tissue spheroids for organ printing. *Procedia CIRP*, 2013, 5: 276–281
  20. R. J. Thomas, et al. The effect of three-dimensional co-culture of hepatocytes and hepatic stellate cells on key hepatocyte functions *in vitro*. *Cells Tissues Organs (Print)*, 2005, 181(2): 67–79
  21. Y. C. Tung, A. Y. Hsiao, S. G. Allen, Y. S. Torisawa, M. Ho, S. Takayama. High-throughput 3D spheroid culture and drug testing using a 384 hanging drop array. *Analyst*, 2011, 136(3): 473–478
  22. G. R. Souza, et al. Three-dimensional tissue culture based on magnetic cell levitation. *Nat. Nanotechnol.*, 2010, 5(4): 291–296
  23. T. Liu, M. Winter, B. Thierry. Quasi-spherical microwells on superhydrophobic substrates for long term culture of multicellular spheroids and high throughput assays. *Biomaterials*, 2014, 35(23): 6060–6068
  24. S. E. Yeon, et al. Application of concave microwells to pancreatic tumor spheroids enabling anticancer drug evaluation in a clinically relevant drug resistance model. *PLoS ONE*, 2013, 8(9): e73345
  25. L. Kang, M. J. Hancock, M. D. Brigham, A. Khademhosseini. Cell confinement in patterned nanoliter droplets in a microwell array by wiping. *J. Biomed. Mater. Res. A*, 2010, 93(2): 547–557
  26. H. Tekin, M. Anaya, M. D. Brigham, C. Nauman, R. Langer, A. Khademhosseini. Stimuli-responsive microwells for formation and retrieval of cell aggregates. *Lab Chip*, 2010, 10(18): 2411–2418
  27. C. Kim, J. H. Bang, Y. E. Kim, S. H. Lee, J. Y. Kang. On-chip anticancer drug test of regular tumor spheroids formed in microwells by a distributive microchannel network. *Lab Chip*, 2012, 12(20): 4135–4142
  28. C. Kim, et al. 3-Dimensional cell culture for on-chip differentiation of stem cells in embryoid body. *Lab Chip*, 2011, 11(5): 874–882
  29. H. C. Moeller, M. K. Mian, S. Shrivastava, B. G. Chung, A. Khademhosseini. A microwell array system for stem cell culture. *Biomaterials*, 2008, 29(6): 752–763
  30. Y. S. Hwang, B. G. Chung, D. Ortmann, N. Hattori, H. C. Moeller, A. Khademhosseini. Microwell-mediated control of embryoid body size regulates embryonic stem cell fate via differential expression of WNT5a and WNT11. *Proc. Natl. Acad. Sci. U.S.A.*, 2009, 106(40): 16978–16983
  31. Y. Xia, G. M. Whitesides. Soft lithography. *Annu. Rev. Mater. Sci.*, 1998, 28(1): 153–184
  32. Y. Y. Choi, B. G. Chung, D. H. Lee, A. Khademhosseini, J. H. Kim, S. H. Lee. Controlled-size embryoid body formation in concave microwell arrays. *Biomaterials*, 2010, 31(15): 4296–4303
  33. A. Y. Hsiao, et al. Microfluidic system for formation of PC-3 prostate cancer co-culture spheroids. *Biomaterials*, 2009, 30(16): 3020–3027